Accepted Manuscript

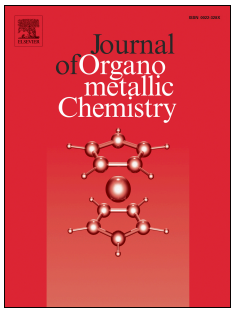

Synthesis of pyridopyrimidinones by N-heterocyclic carbene palladium(II) supported on KCC-1 in aqueous solution

Seyed Mohsen Sadeghzadeh, Rahele Zhiani

PII: S0022-328X(18)30306-1

DOI: 10.1016/j.jorganchem.2018.05.002

Reference: JOM 20435

To appear in: *Journal of Organometallic Chemistry*

Received Date: 24 March 2018

Revised Date: 30 April 2018

Accepted Date: 4 May 2018

Please cite this article as: S.M. Sadeghzadeh, R. Zhiani, Synthesis of pyridopyrimidinones by N-heterocyclic carbene palladium(II) supported on KCC-1 in aqueous solution, *Journal of Organometallic Chemistry* (2018), doi: 10.1016/j.jorganchem.2018.05.002.

Synthesis of pyridopyrimidinones by N-heterocyclic carbene palladium(II) supported on KCC-1 in aqueous solution

Seyed Mohsen Sadeghzadeh*[a,b], Rahele Zhiani[a,b]

[a]*Young Researchers and Elite Club, Neyshabur Branch, Islamic Azad university, P.O. Box 97175-613, Neyshabur, Iran*
[b]*New Materials Technology and Processing Research Center, Department of Chemistry, Neyshabur Branch, Islamic Azad University, Neyshabur, Iran*

Abstract

New *N*, *N'*-substituted imidazolium salts and their corresponding diiodopyridinepalladium(II) complexes were successfully synthesized and supported on KCC-1 (KCC-1/Pd-NHC-Py) has been developed for synthesis of pyridopyrimidinones, providing excellent yields of the corresponding products with remarkable chemoselectivity. This morphology ultimately leads to higher catalytic activity for the KCC-1-supported nanoparticles. The KCC-1/Pd-NHC-Py NPs were thoroughly characterized by using TEM, FESEM, TGA, and BET. We supported a drug on the surface of a silica and used as a catalyst for synthesis another drug.

Keywords: Nano catalyst; Pyridopyrimidinone; One-pot synthesis; Green chemistry; KCC-1

Introduction

Fused N-heterocycles are among the most widely used chemicals owing to its medicinal, [1] agrochemical, [2] and material properties. [3, 4] The 2H-pyridopyrimidinone scaffold is an important class of nitrogen heterocycles. Many synthetic pyridopyrimidinones have occupied privileged position in drug development due to their unprecedented biological activities. This scaffold is an integral part of marketed drugs for the treatment of Schizophrenia [5] and asthma. [6] Many of these molecules have been reported as anticancer, [7] antimalarial, [8, 9] and anticoccidial [10] agents. Some of the them have also been recognized as aldose reductase inhibitors, [11] estrogen-related receptors (ERRs) agonists, [12] G protein signaling (RGS) protein regulators, [13] HIV integrase inhibitors,[14] efflux pump inhibitors,[15] etc.[16] Pyridopyrimidinone scaffold is also a key constituent of numerous natural products possessing wide range of biological activities including antitumor, anti-influenza, oxidative burst inhibitory, lipid droplet synthesis inhibition, and anti-obesity properties. [17-20]

Recently, much attention has been paid to the development of N-heterocyclic carbene metal complexes and remarkable advances have been made especially on their applications as organometallic catalysts. This was attributed to the ability of N-heterocyclic carbene ligands to provide highly active and stable metal complexes for various catalytic applications. The highly sigma donating property of NHC ligands prevents the formation of inactive palladium black during the catalytic reactions. [21-27] Along a similar theme, PEPPSI (Pyridine Enhanced Precatalyst Preparation, Stabilization and Initiation), a term recently coined and demonstrated by Organ and coworkers,[28-31] also resulted in highly active catalysts for various Pd-mediated C–C cross-coupling reactions. [32-34]

Recently, Polshettiwar et al. [35] reported a novel fibrous nanosilica (KCC-1) material, which has special center-radial pore structures with their pore sizes gradually increasing from the center to the surface. KCC-1 material showed high specific surface area due to the pores in the fibers, and the accessibility of the active sites was significantly increased as a result of the special structure. [36-40] Additionally, the 3D architectures generated hierarchical pore structure with macropores can also improve the mass transfer of the reactant. [41-43] The KCC-1-based sorbents may have several advantages over conventional silica-based sorbents, including (i) high catalyst loading, (ii) minimum reduction in surface area after functionalization and (iii) more accessibility of the catalyst sites to enhance the reaction, due to the fibrous structure and highly accessible surface area of KCC-1. Given our continued interest in nanocatalysis and catalyst development for organic reactions, [44-51] we reported the preparation and characterization of palladium (II) complex supported by KCC-1 nanoparticles. In addition, we described its utility for investigate the one-pot synthesis of pyridopyrimidinones, which could be easily separated from the reaction mixture for reuse (Scheme 1).

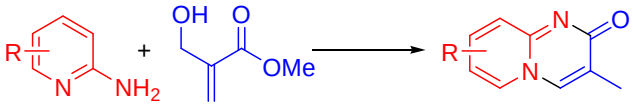

Scheme 1 Synthesis of pyridopyrimidinones in the presence of KCC-1/Pd-NHC-Py NPs.

Experimental

Materials and methods

Chemical materials were purchased from Fluka and Merck in high purity. Melting points were determined in open capillaries using an Electrothermal 9100 apparatus and are uncorrected. FTIR spectra were recorded on a VERTEX 70 spectrometer (Bruker) in the transmission modein spectroscopic grade KBr pellets for all the powders. The particle size and structure of nano particle was observed by using a Philips CM10 transmission electron microscope operating at 100 kV. Powder X-ray diffraction data were obtained using Bruker D8 Advance model with Cu ka radition. The thermogravimetric analysis (TGA) was carried out on a NETZSCH STA449F3 at a heating rate of 10 °C min^{-1} under nitrogen. ^{1}H and ^{13}C NMR spectra were recorded on a BRUKER DRX-300 AVANCE spectrometer at 300.13 and 75.46 MHz, BRUKER DRX-400 AVANCE spectrometer at 400.22 and 100.63 MHz, respectively. Elemental analyses for C, H, and N were performed using a Heraeus CHN–O-Rapid analyzer. The purity determination of the products and reaction monitoring were accomplished by TLC on silica gel polygram SILG/UV 254 plates. Mass spectra were recorded on Shimadzu GCMS-QP5050 Mass Spectrometer.

General procedure for the preparation of KCC-1 NPs

TEOS (2.5 g) was dissolved in a solution of cyclohexane (30 mL) and 1-pentanol (1.5 mL). A stirred solution of cetylpyridinium bromide (CPB 1 g) and urea (0.6 g) in water (30 mL) was then added. The resulting mixture was continually stirred for 45 min at room temperature and then placed in a teflon-sealed hydrothermal reactor and heated 120 °C for 5 h. The silica formed was isolated by centrifugation, washed with deionized water and acetone, and dried in a drying oven. This material was then calcined at 550 °C for 5 h in air.

General procedure for the preparation of KCC-1/3-iodopropylsilane NPs

KCC-1 NPs (2 mmol) and THF (20 mL) were mixed together in a beaker, and then NaH (20 mmol) was dispersed in to the mixture by ultrasonication. 3-iodopropylsilane (22 mmol) was added drop-wise at room temperature and stirred for another 16 h at 60 ^{o}C. The resultant products were collected and washed with ethanol and deionized water in sequence, and then dried under vacuum at 60 ^{o}C for 2 h for further use.

General procedure for the preparation of 5-(4-methoxyphenyl)-1-methyl-1H-imidazole

5-Bromo-1-methyl-1H-imidazole (0.50 mmol), $Pd(PPh_3)_2Cl_2$ (0.025 mmol, 5.0 mol%), K_2CO_3 (1.0 mmol), DMF (2.0 mL), distilled water (2.0 mL) and the (4-methoxyphenyl)boronic acid (0.60 mmol), were added in a 10 mL round bottom flask. The mixture was stirred at 90 ^{o}C for 24 h. After completion of the reaction, the mixture was cooled down to room temperature and extracted 3 times with ethyl acetate. The combined ethyl acetate extract was dried using anhydrous $MgSO_4$. The solvent was removed under reduced pressure and the product was purified by silica gel column chromatography using hexane-ethyl acetate (1:1) followed by 7 % methanol in ethyl acetate as an eluent.

General procedure for the preparation of KCC-1/N-Heterocyclic carbene

5-(4-Methoxyphenyl)-1-methyl-1H-imidazole (0.50 mmol) and KCC-1/3-iodopropylsilane (200 mg) were added into a 10 mL round bottom flask. The mixture was stirred at 100 ^{o}C for 48 hours. The mixture was cooled down to room temperature. Diethyl ether (5 mL) was added and stirred for 15 minutes. The ether was decanted. The product was washed several times with ether. The pure product was dried under vacuum.

General procedure for the preparation of KCC-1/Pd-NHC-Py

N-Heterocyclic carbene ligand precursor (100 mg), palladium(II) iodide (0.50 mmol), potassium carbonate (2.0 mmol) and pyridine (5.0 mL) were added into a 15 mL round bottom flask. The reaction mixture was stirred at 90 ^{o}C for 24 h. The crude product was cooled down to room temperature and diluted with 5 mL dichloromethane. After filtering it, the residue was washed with ethanol again and air-dried at room temperature. Finally, a fine powder was ground out of the resulted complex to be later used as a catalyst.

General procedure for synthesis of pyridopyrimidinones

A mixture of 2-aminopyridine derivative (1.0 mmol) and Baylis-Hillman adducts (1.0 mmol), and KCC-1/Pd-NHC-Py NPs (1 mg) was stirred heating under reflux in TFA (3 mL) for 1 h. The catalyst was separated by filtration. Evaporation of the solvent of the filtrate under reduced pressure gave the crude products. The pure products were isolated by chromatography on silica gel eluted with petroleum ether:EtOAc (3:1).

Results and discussion

The KCC-1 coreeshell was synthesized by a simple method and then functionalized by the N-heterocyclic carbene palladium(II), according to scheme 2. The synthesized KCC-1/Pd-NHC-Py NPs was then characterized by different methods such as TEM, SEM, TGA, and BET (Scheme 2).

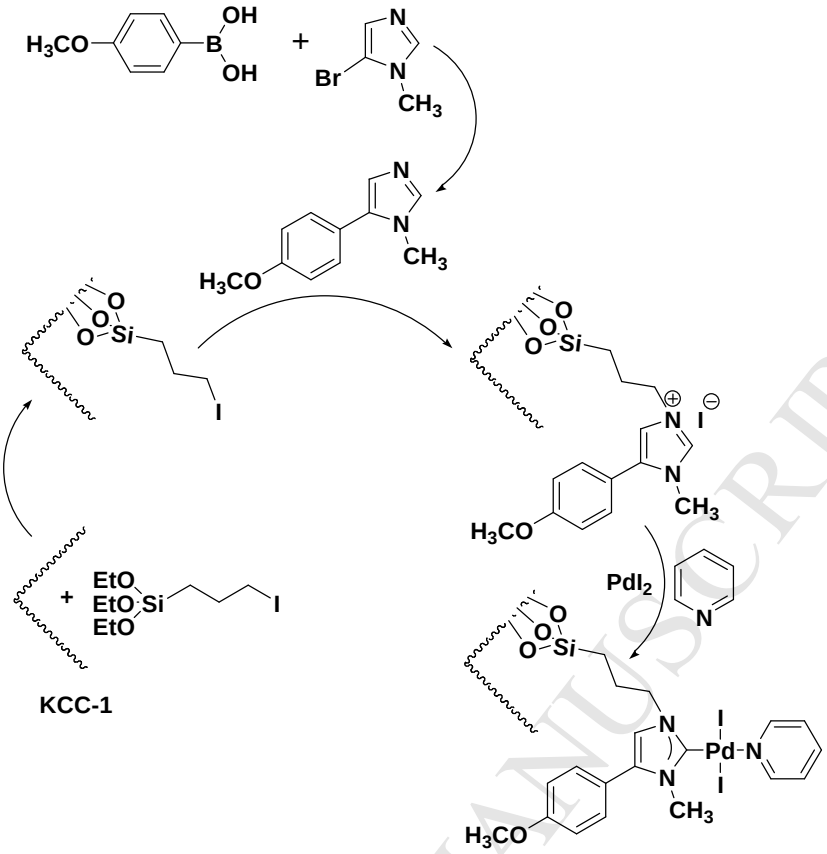

Scheme 2 Schematic illustration of the synthesis for KCC-1/Pd-NHC-Py NPs.

The morphology and structure of the KCC-1 and KCC-1/Pd-NHC-Py NPs are further characterized by FESEM and TEM. Figure 1a shows an FESEM image of highly textured KCC-1 samples, where the samples have spheres of uniform size with diameters of ~300 nm and a wrinkled radial structure. TEM image of KCC-1 shows that wrinkled fibers (with thicknesses of ~8.5 nm) grow out from the center of the spheres and are arranged radially in three dimensions (Figure 1b). Also, the overlapping of the wrinkled radial structure forms cone-shaped open pores. The FESEM and TEM image shows that the entire sphere is solid and composed of fibers. Furthermore, this open hierarchical channel structure and fibers are more easily for the mass transfer of reactants and increase the accessibility of active sites. The FESEM and TEM images of KCC-1/Pd-NHC-Py NPs showed that after modification the morphology of KCC-1 is not change (Figures 1c and 1d).

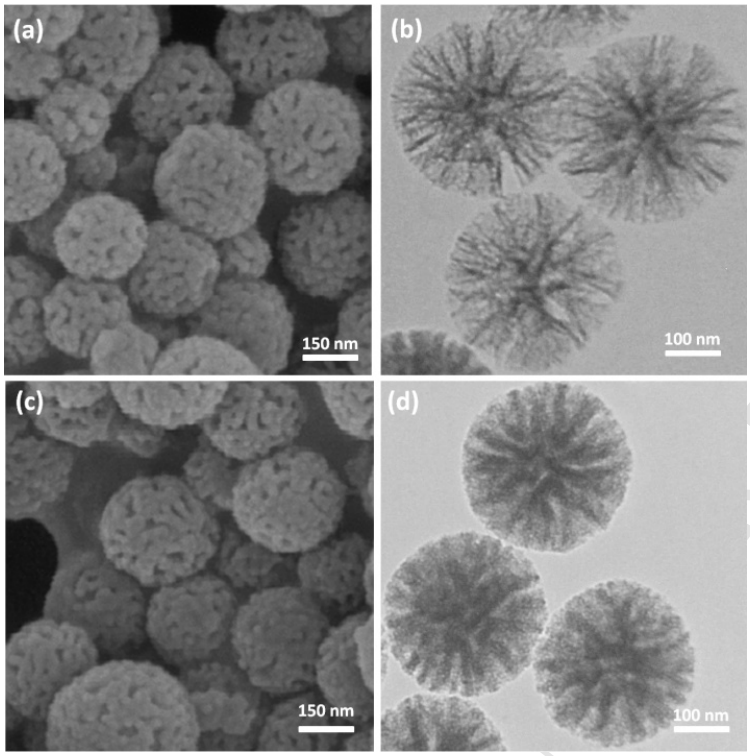

Figure 1 FESEM images of KCC-1 NPs (a); TEM images of KCC-1 NPs (b); FESEM images of KCC-1/Pd-NHC-Py NPs (c); TEM images of KCC-1/Pd-NHC-Py NPs (d).

It was very important to us that the catalyst was stable. The mechanical stability of KCC-1/Pd-NHC-Py NPs was examined using FESEM. The morphology of KCC-1/Pd-NHC-Py NPs remains unaffected even after mechanical compression up to 200 MPa pressure (Figure 2a). Also, we conducted a series of experiments to study the effect of microwave irradiation stabilities on the morphology of KCC-1/Pd-NHC-Py NPs ratios were varied, which isn't affected at power to 650 W (Figure 2b). KCC-1/Pd-NHC-Py NPs also possesses high solvothermal stability, and the structures remained unchanged even after heating in boiling DMSO for 60 h (Figure 2c). The FESEM analysis of KCC-1/Pd-NHC-Py NPs at 1000 ^{o}C showed that it is thermally stable with no visible changes in the morphology and size of the particles (Figure 2d). We did not observe any coagulation of the particles even after severe thermal treatment. This is an interesting perspective, as thermal stability is the significant condition for catalysts operating in highly exothermic media. That way, as-synthesized high-surface-area KCC-1/Pd-NHC-Py NPs have considerable thermal, mechanical, microwave irradiation, and solvothermal stabilities which are necessary attributes for good catalytic support.

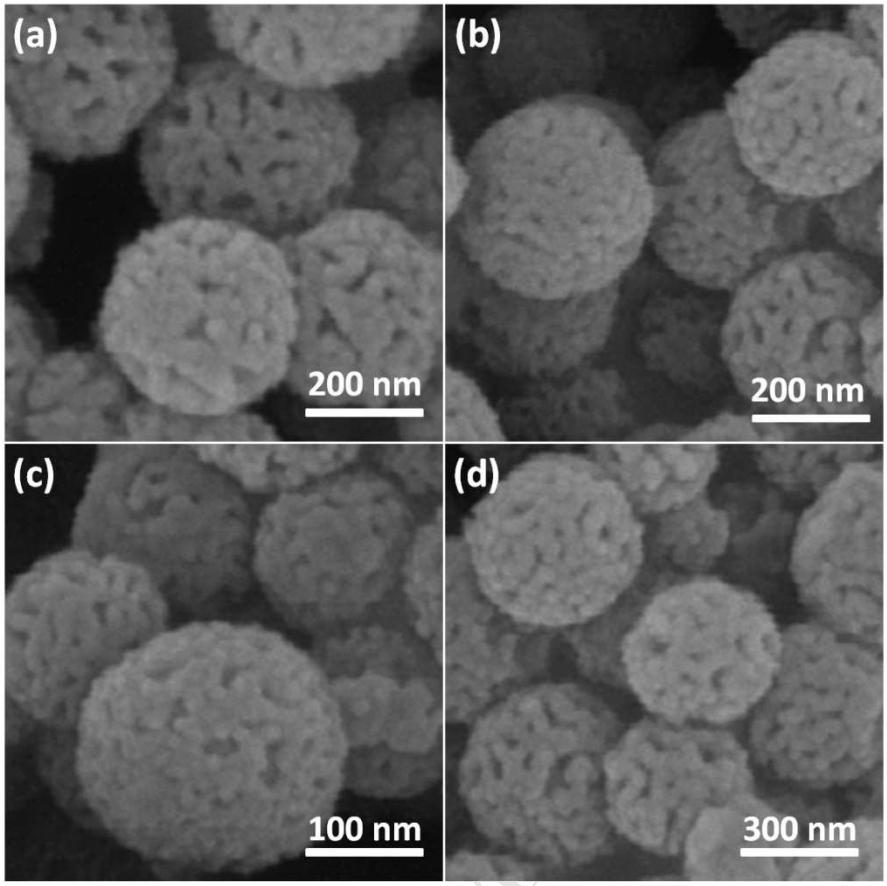

Figure 2 FESEM images of KCC-1/Pd-NHC-Py NPs after mechanical compression at pressures of 200 Mpa (a); after microwave irradiation at power to 650 W (b); after heating in boiling DMSO for 60 h (c); after calcination at 1000 ^{o}C/6 h (d).

The thermal behavior of KCC-1/Pd-NHC-Py NPs is shown in figure 3. The weight loss below 150 ^{o}C was ascribed to the elimination of the physisorbed and chemisorbed solvent on the surface of the KCC-1/Pd-NHC-Py material. In the second stage (180–350 ^{o}C), weight loss is about 33.1 wt%, which can be attributed to the organic group derivatives.

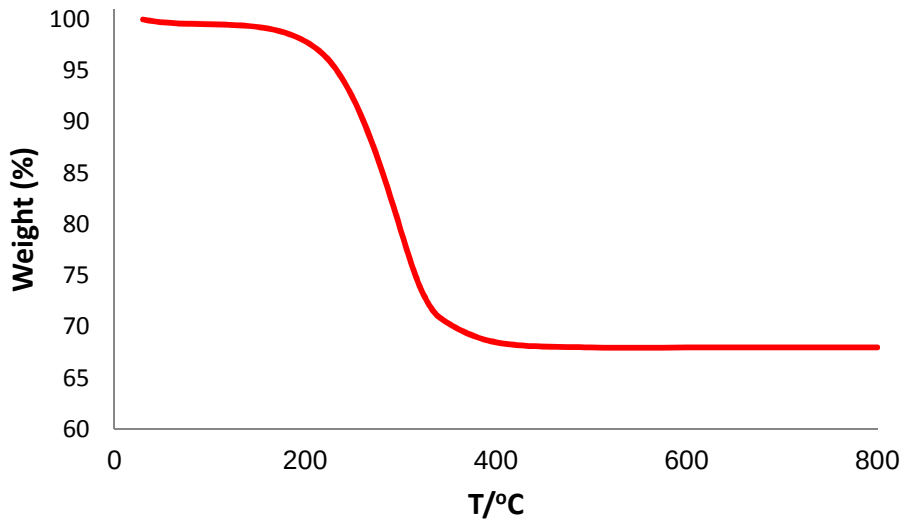

Figure 3 TGA diagram of KCC-1/Pd-NHC-Py NPs.

The N_2 adsorption–desorption isotherms of KCC-1/Pd-NHC-Py NPs showed characteristic type IV curve (Figure 4), which isconsistent with literature reports on standard fibrous silica spheres. As for KCC-1, the BET surface area, total pore volume, and BJH pore diameter are obtained as 439 m^2/g, 1.49 cm^3/g, and 14.78 nm respectively, whereas the corresponding parameters of KCC-1/Pd-NHC-Py NPs have decreased to 372 m^2/g, 1.05 cm^3/g, and 13.03 nm. The nitrogen sorption

analysis of KCC-1/Pd-NHC-Py NPs also confirms a regular and uniform mesostructure with a decrease in surface area, pore diameter and pore volume parameters in comparison with that of pristine KCC-1. With the functionalization by Pd-NHC-Py-Si, the corresponding pore volumes are drastically reduced. This could be ascribed to increased loading with the sensing probe, which occupies a large volume inside the silica spheres (Figure 4 and Table 1).

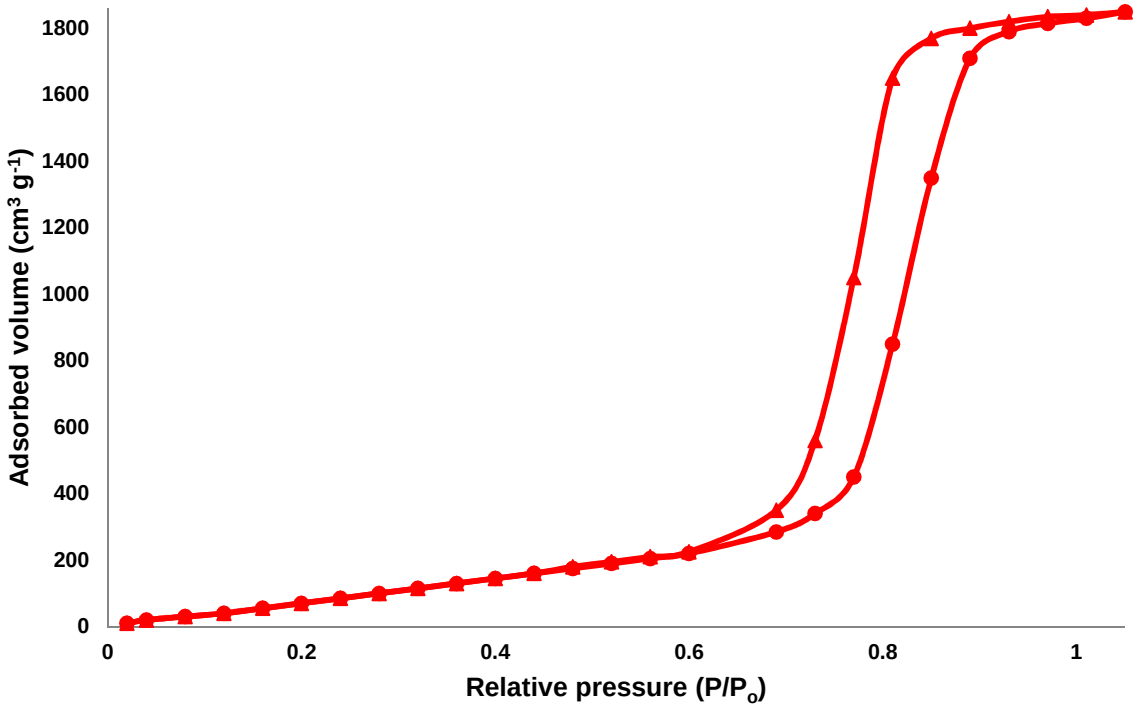

Figure 4 Adsorption–desorption isotherms of KCC-1/Pd-NHC-Py NPs.

Table 1 Structural parameters of KCC-1 and KCC-1/Pd-NHC-Py NPs materials determined from nitrogen sorption experiments.

Catalysts	S_{BET} (m^2 g^{-1})	V_a (cm^3 g^{-1})	D_{BJH} (nm)
KCC-1	439	1.49	14.78
KCC-1/Pd-NHC-Py	372	1.05	13.03

To optimize reaction conditions for the KCC-1/Pd-NHC-Py NPs catalyst system, the effects of various reaction parameters were investigated . We examined the effect of solvent on the synthesis of pyridopyrimidinone using the KCC-1/Pd-NHC-Py NPs at heating under reflux (Table 2). Solvent does affect on catalysts performance. *n*-Hexane, benzene, CCl_4, or cyclohexane, an non-polar solvent, gave pyridopyrimidinone a lower yield (Table 2, entry 13-16). Also, *i*-PrOH, MeOH, EtOH, and H_2O, protic polar solvents, gave also pyridopyrimidinone in low yields (Table 2, entry 17-20). The reaction was do better in aprotic polar solvent. CH_3CN, THF, CH_2Cl_2, DMF, Toluene, Dioxane, $CHCl_3$, EtOAc, and DMSO gave pyridopyrimidinone in average yields (Table 2, entries 4-12). In this study, it was found that THF is a more efficient (Table 2, entry 4) over other solvents. A solvent that stabilizes one of two competing transition states that control the selectivity should enhance the selectivity of the product obtained via the stabilized transition state. We also investigated the crucial role of temperature in the synthesis of pyridopyrimidinone in the presence of KCC-1/Pd-NHC-Py NPs as a catalyst. Results clearly indicated that the catalytic activity is sensitive to reaction temperature. The best temperature for this reaction was at reflux (Table 2, entry 1-4).

Table 2 The effect of solvent and temperature for synthesis of pyridopyrimidinone.[a]

Entry	Solvent	Temp. (˚C)	Yield (%)[b]
1	THF	r.t.	-
2	THF	40	31
3	THF	50	85
4	THF	Reflux	97
5	DMSO	Reflux	41
6	Dioxane	Reflux	33
7	CH_3CN	Reflux	39
8	CH_2Cl_2	Reflux	27
9	EtOAc	Reflux	41
10	DMF	Reflux	25

11	Toluene	Reflux	18
12	$CHCl_3$	Reflux	36
13	*n*-Hexane	Reflux	18
14	Benzene	Reflux	9
15	CCl_4	Reflux	17
16	Cyclohexane	Reflux	12
17	H_2O	Reflux	26
18	EtOH	Reflux	24
19	*i*-PrOH	Reflux	35
20	MeOH	Reflux	22
21	solvent-free	100	-

[a] Reaction conditions: 2-aminopyridine (1 mmol), 2-(hydroxymethyl) acrylate (1 mmol), solvent (10 mL), and catalyst (1 mg), 1 h.
[b] GC yields [%].

As shown in Figure 5, the amount of catalyst also has a significant effect on the coupling reaction. The reaction rate was accelerated quickly in the range 0.8–1.0 mg. However, the yield decreased when the amount of catalyst reached 1.8 mg. Based on these report, it can be inferred that increasing amount of catalyst was propitious to produce pyridopyrimidinone when the amount of catalyst was less than 1.6 mg. Therefore, the amount of catalyst of 1.0 mg was considered as suitable condition.

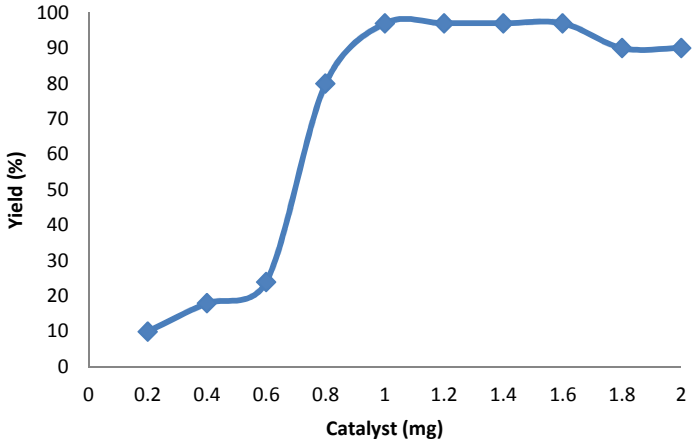

Figure 5 Effect amount of catalyst on yield of pyridopyrimidinone.

The influence of time on this reaction is exhibited in Figure 6. It is obvious that the pyridopyrimidinone yield increased up to 97 % for 60 min. Whereas further increase in the time don't resulted in a slight decrease in the product yield. Therefore, the optimal time for the synthesis of pyridopyrimidinone are 60 min.

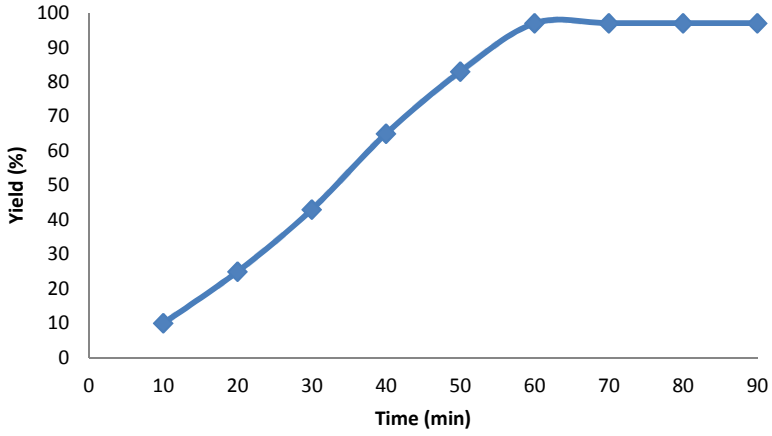

Figure 6 Effect of time on yield of pyridopyrimidinone.

For further investigation the efficiency of the catalyst, different control experiments were performed and the obtained information is shown in Table 3. Initially, a standard reaction was carried out using KCC-1 showed that any amount of the desired product was not formed after 1 h of reaction time (Table 3, entries 1). Also, when KCC-1/*N*-Heterocyclic carbene was used as the catalyst, a reaction was not observed (Table 3, entries 2). The *N*-Heterocyclic carbene group could not give the satisfactory catalytic activity under mild reactions. Based on these disappointing results, we continued the studies to improve the yield of the product by added the Pd-NHC-Py. Notably, there was not much difference in the reaction yields when reaction was carried out using KCC-1/Pd-NHC-Py NPs and Pd-NHC-Py catalyst (Table 3, entries 3 and 7), however, Pd-NHC-Py is not recoverable and reusable for the next runs. These observations show that the reaction cycle is mainly catalyzed by Pd-NHC-Py on the KCC-1 nanostructure. The nano-sized particles increase the exposed surface area of the active site of the catalyst, thereby enhancing the contact between reactants and catalyst dramatically and mimicking the homogeneous catalysts. As a result, KCC-1/Pd-NHC-Py NPs was used in the subsequent investigations because of its high reactivity, high selectivity and easy separation. Also, the activity and selectivity of nano-catalyst can be manipulated by tailoring chemical and physical properties like size, shape, composition and morphology. To assess the exact impact of the presence of KCC-1 in the catalyst, the KCC-1/Pd-NHC-Py NPs compared with MCM-41/Pd-NHC-Py, SBA-15/Pd-NHC-Py, and nano-SiO_2/Pd-NHC-Py. When nano-SiO_2/Pd-NHC-Py, MCM-41/Pd-NHC-Py or SBA-15/Pd-NHC-Py was used as the catalyst, the yield of the desired product was average to good, but the yield for KCC-1/Pd-NHC-Py was excellent. Non-negligible activity of the silica was attributed to its shape, composition and morphology. Besides, the large space between fibers can significantly increase the accessibility of the active sites of the KCC-1.That is why, the KCC-1 was more effective than nano-SiO_2, MCM-41, and SBA-15 (Table 3, entries 3-6). As a result, KCC-1 NPs were used in the subsequent investigations because of its high reactivity, high selectivity and easy separation (Table 3).

Table 3 Influence of different catalysts for synthesis of pyridopyrimidinone.[a]

Entry	Catalyst	Yield (%)[b]
1	KCC-1	-
2	KCC-1/*N*-Heterocyclic carbene	-
3	KCC-1/Pd-NHC-Py	97
4	Nano-SiO_2/Pd-NHC-Py	59
5	MCM-41/Pd-NHC-Py	89
6	SBA-15/Pd-NHC-Py	82
7	Pd-NHC-Py	98

[a]Reaction conditions: 2-aminopyridine (1 mmol), 2-(hydroxymethyl) acrylate (1 mmol), TFA (3 mL), and catalyst (1 mg), 1 h.
[b]Isolated yield.

To examine the scope of the catalytic properties of the catalyst for synthesis of pyridopyrimidinone derivatives, various types of aminopyridines were reacted with Baylis-Hillman adducts in the presence of a catalytic amount of KCC-1/Pd-NHC-Py NPs. It was found that all aminopyridines and Baylis-Hillman adducts were suitable for this reaction, giving the desired products excellent yields (Table 4).

Table 4 Synthesis of pyridopyrimidinone derivatives in the presence of KCC-1/Pd-NHC-Py NPs.[a]

Entry	Aminopyridines	BH adducts	Product	Yield (%)[b]
1	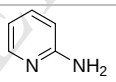	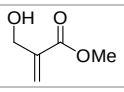	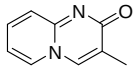	96
2	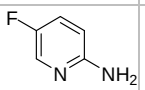	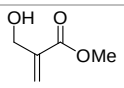	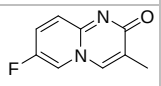	90
3	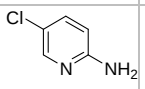	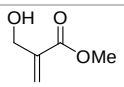	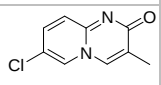	92
4	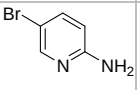	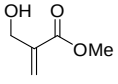	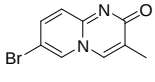	94
5	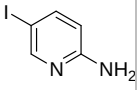	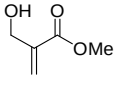	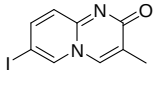	91
6	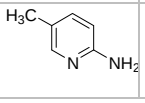	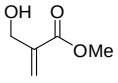	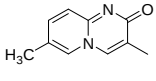	97

7	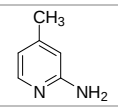	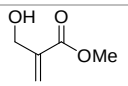	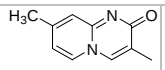	95
8	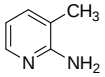	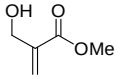	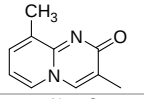	96
9	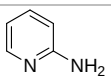	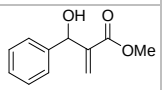	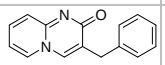	98
10	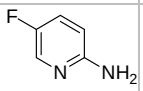	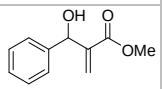	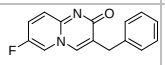	92
11	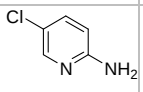	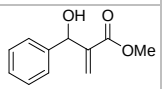	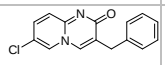	94
12	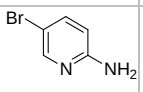	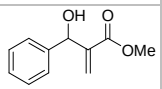	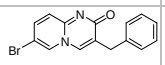	95
13	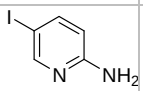	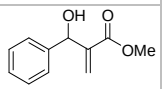	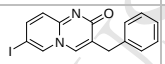	95
14	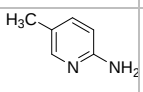	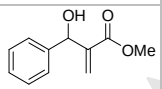	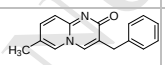	94
15	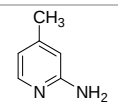	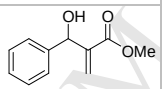	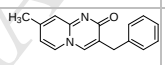	95
16	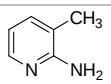	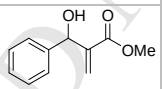	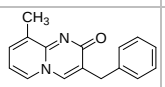	96

[a] Reaction conditions: aminopyridines (1 mmol), Baylis-Hillman adducts (1 mmol), TFA (3 mL), and catalyst (1 mg), 1 h.
[b]Isolated yield.

It is important to note that the heterogeneous property of KCC-1/Pd-NHC-Py NPs facilitates its efficient recovery from the reaction mixture during work-up procedure. The activity of the recycled catalyst was also examined under the optimized conditions. After the completion of reaction, the catalyst was separated by filtration, washed with methanol and dried at the pump. The recovered catalyst was reused for ten consecutive cycles without any significant loss in catalytic activity (Figure 7).This lack of reduction in catalyst performance can be attributed to the simple and stability of the catalyst structure. The lack of any reduced performance of the catalyst could be related to its simple and stable structure. Pd (II) leaching was studied by inductively coupled plasma mass spectrometry (ICP-MS) analysis of the catalyst, after ten cycles of reactions. The contents of Pd (II) in catalyst before and after reaction were 4.9 % and 4.7 % respectively, determined by ICP-MS. These indicate that most of Pd (II) species leaching into solution are recaptured onto the fibers of KCC-1 after completion of the reaction. It is important to note that the heterogeneous property of KCC-1/Pd-NHC-Py NPs facilitates its efficient recovery from the reaction mixture after the completion of reaction (Table 5).

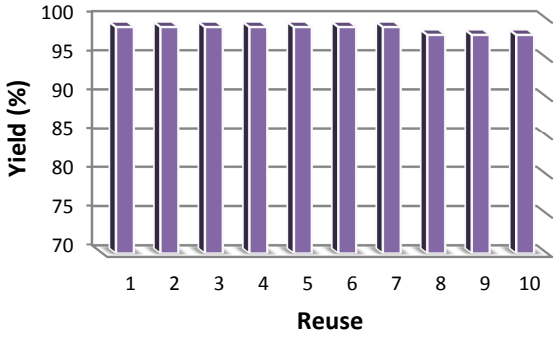

Figure 7 The reusability of catalysts for synthesis of pyridopyrimidinone.

Table 5 The loading amount of Pd (II).

Entry	Catalyst	wt %
1	KCC-1/Pd-NHC-Py	4.9
2	KCC-1/Pd-NHC-Py after ten reuses	4.7

Conclusions

In the present study KCC-1/Pd-NHC-Py NPs was synthesized and characterized as an environmentally-friendly nanocatalyst for the synthesis of pyridopyrimidinones with various electronically diverse substrates. The experimental results displayed the core-shell structure of the synthesized catalyst with a mean size range of 250-300 nm. In addition, the catalyst was easily recoverable and reusable. Subsequently, high yields in short reaction times were achieved without the need for a pyridopyrimidinone catalyst as well as excellent reusability for at least ten times in the corresponding reaction without a reduction in catalytic activity.

Notes and references

1 J. J. Li, Heterocyclic chemistry in drug discovery, John Wiley & Sons, Hoboken, N.J., (2013).
2 S. Jeanmart, A. J. Edmunds, C. Lamberth and M. Pouliot, Bioorg. Med. Chem., 24 (2016) 317-341.
3 D. C. Chen, S. J. Su and Y. Cao, J Mater Chem C, 2 (2014) 9565-9578.
4 M. Liu, S. J. Su, M. C. Jung, Y. B. Qi, W. M. Zhao and J. Kido, Chem Mater, 24 (2012) 3817-3827.
5 M. Corena-McLeod, Drugs R D, 15 (2015) 163-174.
6 T. Gohda, C. Ra, C. Hamada, T. Tsuge, H. Kawachi and Y. Tomino, Arzneimittelforschung, 58 (2008) 18-23.
7 J. Ni, Q. S. Liu, S. Z. Xie, C. Carlson, T. Von, K. Vogel, S. Riddle, C. Benes, M. Eck, T. Roberts, N. Gray and J. Zhao, Cancer Discov, 2 (2012) 425-433.
8 U. R. Mane, D. Mohanakrishnan, D. Sahal, P. R. Murumkar, R. Giridhar and M. R. Yadav, Eur. J. Med. Chem., 79 (2014) 422-435.
9 U. R. Mane, H. Li, J. Huang, R. C. Gupta, S. S. Nadkarni, R. Giridhar, P. P. Naik and M. R. Yadav, Bioorg. Med. Chem., 20 (2012) 6296-6304.
10 L. Silpa, A. Niepceron, F. Laurent, F. Brossier, M. Penichon, C. Enguehard-Gueiffier, M. Abarbri, A. Silvestre and J. Petrignet, Bioorg. Med. Chem. Lett., 26 (2016) 114-120.
11 C. La Motta, S. Sartini, L. Mugnaini, F. Simorini, S. Taliani, S. Salerno, A. M. Marini, F. Da Settimo, A. Lavecchia, E. Novellino, M. Cantore, P. Failli and M. Ciuffi, J Med Chem, 50 (2007) 4917-4927.
12 L. Peng, X. Gao, L. Duan, X. Ren, D. Wu and K. Ding, J Med Chem, 54 (2011) 7729-7733.
13 L. L. Blazer, D. L. Roman, A. Chung, M. J. Larsen, B. M. Greedy, S. M. Husbands and R. R. Neubig, Mol. Pharmacol., 78 (2010) 524-533.
14 G. Le, N. Vandegraaff, D. I. Rhodes, E. D. Jones, J. A. Coates, L. Lu, X. Li, C. Yu, X. Feng and J. J. Deadman, Bioorg. Med. Chem. Lett., 20 (2010) 5013-5018.
15 M. Askoura, W. Mottawea, T. Abujamel and I. Taher, Libyan J Med, (2011) 6.
16 S. Rapolu, M. Alla, R. J. Ganji, V. Saddanapu, C. Kishor, V. R. Bommena and A. Addlagatta, Med. Chem. Comm., 4 (2013) 817-821.
17 G. Yu, G. Zhou, M. Zhu, W. Wang, T. Zhu, Q. Gu and D. Li, Org. Lett., 18 (2016) 244-247.
18 J. F. Rebhun, S. J. Roloff, R. A. Velliquette and S. R. Missler, Fitoterapia, 101 (2015) 57-63.
19 G. Huang, D. Roos, P. Stadtmüller and M. Decker, Tetrahedron Lett, 55 (2014) 3607-3609.
20 A. Schramm and M. Hamburger, Fitoterapia, 94 (2014) 127-133.
21 F. Rajabi, W. R. Thiel Adv, Synth. Catal. 356 (2014) 1873 – 1877.
22 C. Zhang, J. Liu, C. Xia, Org. Biomol. Chem. 12 (2014) 9702.
23 A. Chartoire, A. Boreux, A. R. Martin, S. P. Nolan, RSC Advances 3 (2013) 3840.
24 T. Wang, H. Xie, L. Liu, W.X. Zhao, Journal of Organometallic Chemistry 804 (2016) 73-79.
25 K. Natte, J. Chen, H. Neumann, M. Beller, X. Wu, Org. Biomol. Chem., 12 (2014) 5590.
26 A. Chartoire, X. Frogneux, S. P. Nolan, Adv. Synth. Catal. 354 (2012) 1897–1901.

27 V. H. Nguyen, M. B. Ibrahim, W. W. Mansour, B. M. El Ali, H. V. Huynh, Organometallics 36 (2017) 2345−2353.
28 C. J. O'Brien, E. A. B. Kantachev, G. A. Chass, N. Hadei, A. C. Hopkinson, M. G. Organ, D. H. Setaidi, T.-H. Tang, D.-C. Fang, Tetrahedron, 61 (2005) 9723–9735.
29 M. G. Organ, S. Avola, I. Dubovyk, N. Hadei, A. S. B. Kantchev, C. J. O'Brien, C. Valente, Chem. Eur. J., 12 (2006) 4749–4755.
30 M. G. Organ, M. Abdel-Hadi, S. Avola, N. H. Nasielski, C. J. O'Brien, C. Valente, Chem. Eur. J., 13 (2007) 150–157.
31 C. J. O'Brien, E. A. B. Kantachev, C. Valente, N Hadei, G. A. Chass, A. Lough, A. C. Hopkinson, M. G. Organ, Chem. Eur. J., 12 (2006) 4743–4748.
32 C. J. O'Brien, E. A. Kantchev, C. Valente, M Hadei, G. Chas, A. Lough, A. C. Hopkinson, M. G. Organ, Chem. Eur. J. 12 (2006) 4743-4748.
33 M. G. Organ, S. Avola, I. Dubovyk, N. Hadei, E. A. B. Kantchev, C. J. O'Brien, C. Valente, Chem. Eur. J. 12 (2006) 4749–4755.
34 C. Valente, M. E. Belowich, N. Hadei, M. G. Organ, Eur. J. Org. Chem. (2010) 4343–4748.
35 V. Polshettiwar, D. Cha, X. Zhang, J. M. Basset, Angew. Chem., 49 (2010) 9652–9656.
36 A. Maity, V. Polshettiwar, ChemSusChem 10 (2017) 3866–3913.
37 P.K. Kundu, M. Dhiman, A. Modak, A. Chowdhury, V. Polshettiwar, ChemPlusChem, 81 (2016) 1142–1146.
38 P. Gautam, M. Dhiman, V. Polshettiwar, B. M. Bhanage, Green Chem., 18 (2016) 5890-5899.
39 A. Fihri, D. Cha, M. Bouhrara, N. Almana, V. Polshettiwar, ChemSusChem, 5 (2012) 85–89.
40 A. Fihri, M. Bouhrara, U. Patil, D. Cha, Y. Saih, V. Polshettiwar, ACS Catal., 2 (2012) 1425–1431.
41 A. S. Lilly Thankamony, C. Lion, F. Pourpoint, B. Singh, A. J. Perez Linde, D. Carnevale, G. Bodenhausen, H. Vezin, O. Lafon, V. Polshettiwar, Angew. Chem., 54 (2015) 2190–2193.
42 N. D. Petkovich, A. Stein, Chem. Soc. Rev., 42 (2013) 3721–3739.
43 C. M. Parlett, K. Wilson, A. F. Lee, Chem. Soc. Rev., 42 (2013) 3876–3893.
44 S.M. Sadeghzadeh, R. Zhiani, S. Emrani, M. Ghabdian, RSC Adv., 7 (2017) 50838–50843.
45 S.M. Sadeghzadeh, R. Zhiani, M. Khoobi, S. Emrani, Microporous and Mesoporous Materials 257 (2018) 147-153.
46 S.M. Sadeghzadeh, Microporous and Mesoporous Materials 234 (2016) 310-316.
47 S.M. Sadeghzadeh, Journal of Molecular Liquids 223 (2016) 267–273.
48 S.M. Sadeghzadeh, Journal of Molecular Catalysis A: Chemical 423 (2016) 216–223.
49 S.M. Sdeghzadeh, Catal. Sci. Technol., 6 (2016) 1435–1441.
50 S.M. Sadeghzadeh, Catal. Commun., 72 (2015) 91–96.
51 S.M. Sadeghzadeh, Green Chem., 17 (2015) 3059–3066.

Highlights

1- An efficient *N*, *N'*-substituted imidazolium salts and their corresponding diiodopyridinepalladium(II) complexes supported on KCC-1 (KCC-1/Pd-NHC-Py) has been developed.

2- The KCC-1/Pd-NHC-Py NPs were thoroughly characterized by using TEM, FESEM, TGA, and BET.

3- High catalytic activity and ease of recovery from the reaction mixture by filtration.